Available online at www.derpharmachemica.com

Scholars Research Library

Der Pharma Chemica, 2012, 4(4):1759-1768
(http://derpharmachemica.com/archive.html)

ISSN 0975-413X
CODEN (USA): PCHHAX

On the adsorption properties of an imidazole-pyridine derivative as corrosion inhibitor of mild steel in 1 M HCl

O. El Khattabi[1], **B. Zerga**[2], **M. Sfaira**[2*], **M. Taleb**[2], **M. Ebn Touhami**[1],
B. Hammouti[3], **L. Herrag**[3], **M. Mcharfi**[2]

[1] Laboratoire des Matériaux, Electrochimie et Environnement, Faculté des Sciences, Université Ibn Tofaîl, BP. 133 – 14000, Kénitra, Morocco
[2] Laboratoire d'Ingénierie des Matériaux, de Modélisation et d'Environnement, LIMME, Faculté des Sciences Dhar El Mahraz, Université Sidi Mohammed Ben Abdellah, USMBA, BP 1796 – 30000, Atlas – Fès, Morocco
[3] LCAE-URAC18, Faculté des Sciences, Université Mohammed Premier, BP 717 – 60000, Oujda, Morocco

---

Abstract

The inhibition effect of a new imidazolpyridine derivative namely 2,6-bis(2,5-dimethyl-2H-imidazol-4-yl)pyridine (BDIP) on corrosion of mild steel in 1 M HCl was studied at 308 K. Weight-loss measurements, potentiodynamic polarisation and impedance spectroscopy (EIS) methods were used. Results showed that BDIP was a good inhibitor and its inhibiting efficiency reaches 97,4% at 10^{-3} *M. The values of the inhibition efficiency calculated from these techniques are reasonably in good agreement. Polarisation curves revealed that this organic compound acted predominately as a cathodic inhibitor. EIS measurements showed that the charge transfer resistance increases with the inhibitor concentration. The temperature effect on the corrosion behaviour of mild steel in 1 M HCl with and without BDIP at* 10^{-3} *M was studied in the temperature range 308–353 K. The associated activation energy was determined. The adsorption of BDIP on the mild steel surface obeyed to the Langmuir's adsorption isotherm model.*

Keywords: Corrosion; Mild steel; imidazolpyridine; Inhibition; Hydrochloric acid

---

INTRODUCTION

The corrosion of metals is a fundamental academic as well as an industrial concern which has received a considerable amount of attention [1]. Acid solutions are generally used for the removal of rust and scale in several industrial processes. In particularity, HCl is widely used in the pickling of mild steel and ferrous alloys. Inhibitors are generally used in these processes to control metal dissolution [2]. Many *N*-heterocyclic compounds with polar groups and/or π-electrons are efficient inhibitors of the corrosion of mild steel and iron in acidic media [3-6]. This kind of organic molecules can adsorb on the metal surface because it can form bonds between the *N* electron lone pair and/or the π-electron cloud with the metal and thereby reducing the corrosive attack on metals in acidic media [2,3]. This behaviour is influenced by the nature and surface charge of metal, by the type of aggressive electrolyte and by the chemical structure of inhibitors [7]. It is well recognized that pyrazole [8-11], bipyrazole [12-17], tripyrazole [18], triazole [19-25] and tetrazole [26-29] derivative compounds are excellent inhibitors of corrosion for many metals and alloys in aggressive media.

The aim of this paper was to study the inhibiting action of a new imidazolyrazolic compound, namely 2,6-bis(2,5-dimethyl-2H-imidazol-4-yl)pyridine and denoted hereafter BDIP. The anticorrosion behaviour of mild steel in HCl medium in the absence and presence of BDIP inhibitor has been studied by gravimetric method and electrochemical techniques such as potentiodynamic polarisation and impedance spectroscopy (EIS). The thermodynamic parameters of BDIP molecule adsorption onto mild steel were determined and the nature of inhibitor adsorption process was also studied and discussed.

MATERIALS AND METHODS

2. EXPERIMENTAL PROCEDURE

2.1. Synthesis of the 2,6-bis(2,5-dimethyl-2H-imidazol-4-yl)pyridine compound

The organic compound BDIP under study was synthesised through the reaction as shown in Scheme 1, purified and characterized by infra-red, ^{1}H nuclear magnetic resonance (NMR) spectroscopic methods and microanalysis before use. BDIP was thereafter tested as corrosion inhibitor of mild steel in hydrochloric solution. The molecular structure of the newly studied inhibitor is shown in Scheme 1. The choice of this compound is based on molecular structure considerations; the presence of nitrogen atoms and aromatic rings are likely to facilitate the adsorption of the compound on the metal surface.

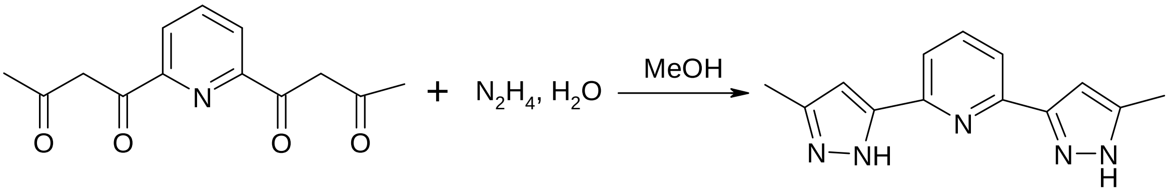

Scheme 1: Synthesis route and chemical formula of the new synthesized BDIP

2.2. Gravimetric measurements

The aggressive solution (1 M HCl) was prepared by dilution of analytical grade 37% HCl with double-distilled water. Prior to all measurements, the mild steel samples (0.09% P; 0.38% Si; 0.01% Al; 0.05% Mn; 0.21% C; 0.05% S and the remainder iron) were polished with different emery paper up to 1200 grade, washed thoroughly with double-distilled water, degreased with AR grade ethanol, acetone and dried at room temperature.

Gravimetric measurements were carried out in a double walled glass cell equipped with a thermostat-cooling condenser. The solution volume was 100 mL. The mild steel specimens used had a square form (2 cm × 2 cm × 0.05 cm). The immersion time for the weight loss was 6 h at 308 K. After the corrosion test, the specimens of mild steel were carefully washed in double-distilled water, dried and then weighted. Duplicate experiments were performed in each case and the mean value of the weight loss is reported. Weight loss allowed us to calculate the mean corrosion rate as expressed in mg cm^{-2} h^{-1}.

2.3. Potentiodynamic polarisation measurements

Electrochemical measurements were carried out in a conventional three-electrode electrolysis cylindrical Pyrex glass cell. The working electrode (WE) in the form of a disc cut from mild steel has a geometric area of 1 cm^2 and is embedded in polytetrafluoroethylene (PTFE). A saturated calomel electrode (SCE) and a disc platinum electrode were used as reference and auxiliary electrodes, respectively. The temperature was thermostatically controlled at 308 ± 1 K. The WE was abraded with silicon carbide paper up to grade 1200, degreased with ethanol and acetone, and rinsed with double-distilled water before use.

The polarisation curves were recorded with a digital potentiostat type Voltalab PGZ 100 and controlled with analysis software (Voltamaster 4), at scan rate of 1 mV s^{-1}. The mild steel electrode was maintained at open circuit conditions (corrosion potential, E_{corr}) for 30 min and thereafter pre-polarized at -800 mV for 10 min. After this scan, the potential was swept to more positive values of anodic potentials.

2.4. EIS measurements

The electrochemical impedance spectroscopy (EIS) measurements were performed using a transfer function analyser (Voltalab PGZ 100), with a small amplitude a.c. signal (10 mV rms) over a frequency domain from 100 kHz to 10 mHz at 308 K with 5 points per decade. Computer programs automatically controlled the measurements performed at rest potentials after 30 min of immersion at E_{corr}. The impedance diagrams were given in the Nyquist representation.

RESULTS

3.1. Weight-loss tests

The corrosion rate (W_{corr}) of mild steel in 1 M HCl at different concentrations of BDIP is determined after 6 h of immersion at 308 K. The values of corrosion rates and inhibition efficiencies are given in Table 1. The inhibition efficiency (E_{WL} %) is determined by the following relation (1):

$$E_{WL}\% = \frac{W_{corr} - W_{corr/inh}}{W_{corr}} \times 100 \qquad (1)$$

W_{corr} and $W_{corr/inh}$ are the corrosion rates of mild steel in the absence and the presence of BDIP organic compound, respectively.

Table 1: Gravimetric results of mild steel without and with addition of BDIP at different concentrations at 308 K after 6 h of immersion in 1 M HCl solution

Inhibitor	Concentration C / mol L^{-1}	Corrosion weight loss W_{corr} / mg cm^{-2} h^{-1}	E_{WL} %	Surface coverage θ
Blank	00	1,76	-	0
BDIP	10^{-6}	0.68	61.4	0.6316
	10^{-5}	0.34	80.7	0.8304
	5×10^{-5}	0.18	89.8	0.9240
	10^{-4}	0.10	94.4	0.9708
	5×10^{-4}	0.07	96.1	0.9883
	10^{-3}	0.05	97.4	1

3.2. Polarisation measurements

Current potential characteristics resulting from cathodic polarisation curves of mild steel in molar HCl at various concentrations of the tested BDIP are evaluated. Figure 1 shows typical cathodic Tafel plots of the BDIP at different concentrations.

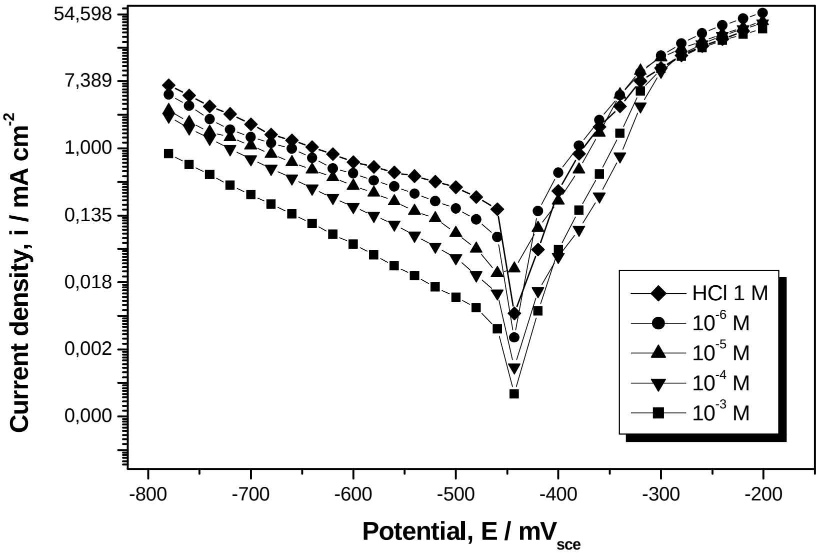

Figure 1: Cathodic and anodic plots of mild steel in 1 M HCl at different concentrations of BDIP

Table 2 collects the corrosion kinetic parameters such as E_{corr}, i_{corr} and β_c obtained from potentiodynamic polarisation curves for mild steel in 1 M HCl containing different concentrations of BDIP. In the case of the steady-state current-voltage (I-E) method determining inhibition efficiency (E_{I-E} %) is done by equation (2):

$$E_{I-E}\% = \frac{i^0_{corr} - i_{corr}}{i^0_{corr}} \times 100 \qquad (2)$$

i^0_{corr} and i_{corr} are the corrosion current densities values without and with BDIP, respectively determined by the extrapolation of cathodic Tafel lines to the corresponding corrosion potential.

Table 2: Values of electrochemical parameters evaluated from the cathodic current-voltage characteristics for the system electrode/1 M HCl with and without added BDIP inhibitor at 308 K

Inhibitor	Concentration C/ mol L^{-1}	E_{corr} mV$_{sce}$	$\lvert \beta_c \rvert$ mV dec^{-1}	i_{corr} µA cm^{-2}	E_{I-E} %
Blank	00	-450	208	144	-
BDIP	10^{-6}	-447	206	70	52
	10^{-5}	-448	184	42	71
	10^{-4}	-450	152	20	87
	10^{-3}	-450	165	10	93

3.3. Electrochemical impedance spectroscopy (EIS) measurements

The corrosion behaviour of mild steel in 1 M hydrochloric acidic solution, in the absence and presence of BDIP, is also investigated by the electrochemical impedance spectroscopy (EIS). Impedance diagrams are obtained for the frequency range 100 KHz–10 mHz at the open circuit potential at 308 K after 30 min of immersion at E_{corr}. Nyquist diagrams for mild steel in 1 M HCl at different concentrations of BDIP are presented in Figure 2.

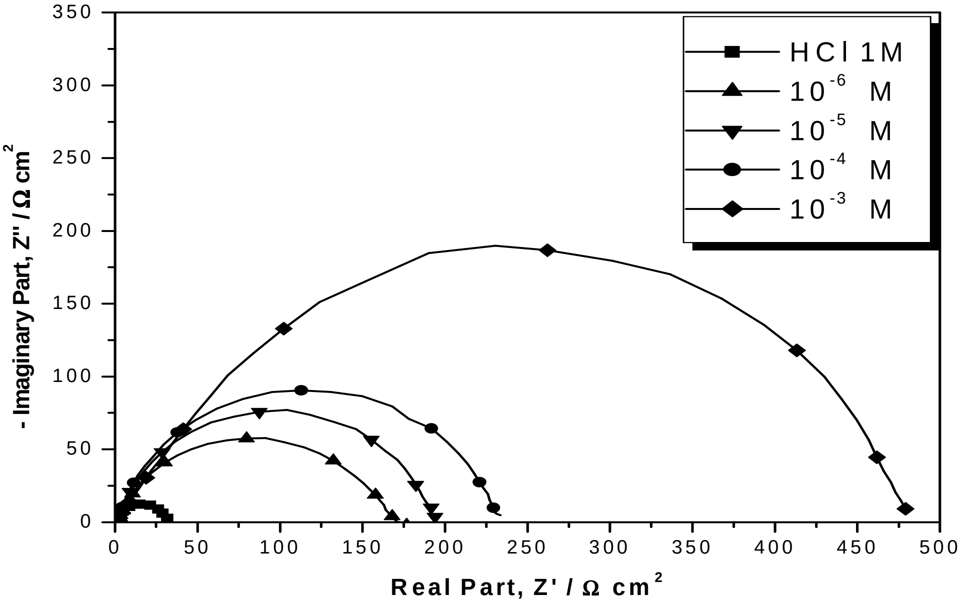

Figure 2: Nyquist plots of mild steel in 1 M HCl containing different concentrations of BDIP

The impedance diagrams consist of one large capacitive loop and they are not perfect semicircles and this difference is generally attributed to the frequency dispersion [30].

The charge-transfer resistance (R_{ct}) values are calculated from the difference in impedance at lower and higher frequencies, as suggested by Tsurus et al. [31]. The double-layer capacitance values (C_{dl}) are derived from the frequency at which the imaginary component of the impedance is maximal ($-Z''_{max}$) as given in the equation (3):

$$C_{dl} = \frac{1}{\omega_{max} R_{ct}} \quad where\ \omega_{max} = 2\pi f_{max} \qquad (3)$$

Table 3 collects the values of the charge-transfer resistance, R_{ct}, the double-layer capacitance, C_{dl} derived from Nyquist plots and the corresponding inhibition efficiency. The inhibition efficiency derived from EIS measurements (E_{imp}%) is defined as follows, equation (4):

$$E_{imp}\% = \frac{R_{ct} - R^0_{ct}}{R_{ct}} \times 100 \qquad (4)$$

R_{ct} and $R°_{ct}$ are the charge transfer resistances with and without the studied BDIP inhibitor, respectively.

Table 3: EIS data of mild steel in 1 M HCl containing different concentrations of the studied BDIP inhibitor at 308 K

Inhibitor	Concentration C/ mol L^{-1}	R_{ct} Ω cm^2	C_{dl} µF cm^{-2}	E_{imp} %
Blank	00	32	160	–
BDIP	10^{-6}	169	45	81
	10^{-5}	195	33	84
	10^{-4}	228	28	86
	10^{-3}	479	11	94

3.4. Effect of temperature

Temperature has a great effect on the corrosion phenomenon. Generally the corrosion rate increases with the rise of temperature. For this purpose, weight-loss measurements were made in the range of temperature from 313 to 353 K, in the absence and presence of BDIP at 10^{-3}M after 1 h of immersion. The corresponding data are shown in Table 4.

Table 4: Influence of temperature on the corrosion rate of mild steel in the presence and absence of 10^{-3} M of BDIP

Temperature T / K	Corrosion weight loss without BDIP $W°_{corr}$ / mg cm^{-2} h^{-1}	Corrosion weight loss with 10^{-3} M of BDIP W_{corr} / mg cm^{-2} h^{-1}	E_{WL} %
313	2.12	0.06	97.2
323	3.52	0.22	93.8
333	6.92	0.38	94.5
343	13.38	0.85	93.7
353	22.95	1.74	92.1

To calculate activation kinetic and thermodynamic parameters of the corrosion reaction such as the energy E_a, the entropy ΔS^* and the enthalpy ΔH^* of activation, Arrhenius equation (5) and its alternative formula called transition state equation (6) were used:

$$W_{corr} = A\exp(-\frac{E_a}{RT}) \tag{5}$$

$$W_{corr} = \frac{RT}{Nh}\exp(\frac{\Delta S^*}{R})\exp(-\frac{\Delta H^*}{RT}) \tag{6}$$

Where T is the absolute temperature in Kelvin, R is the universal gas constant, h is Plank's constant, N is Avogadro's number.

The logarithm of the corrosion rate of mild steel W_{corr} can be represented as straight-lines as a function of $1/T$ (Arrhenius equation) in Figure 3. The activation energy could be determined from the slope of Arrhenius plots for mild steel corrosion process. Plots of $\ln(W_{corr}/T)$ vs. $1/T$ give a straight line with a slope of $\Delta H^*/R$ and an intercept of $(\ln(R/Nh) + \Delta S^*/R)$ as shown in Figure 4.

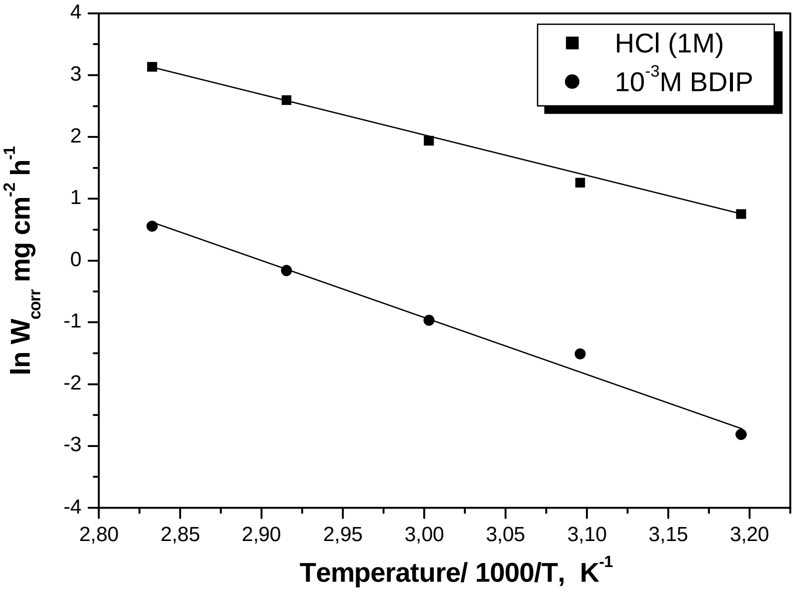

Figure 3: Arrhenius plots for lnW_{corr} vs. 1/T for mild steel in 1 M HCl at 10^{-3} M of BDIP

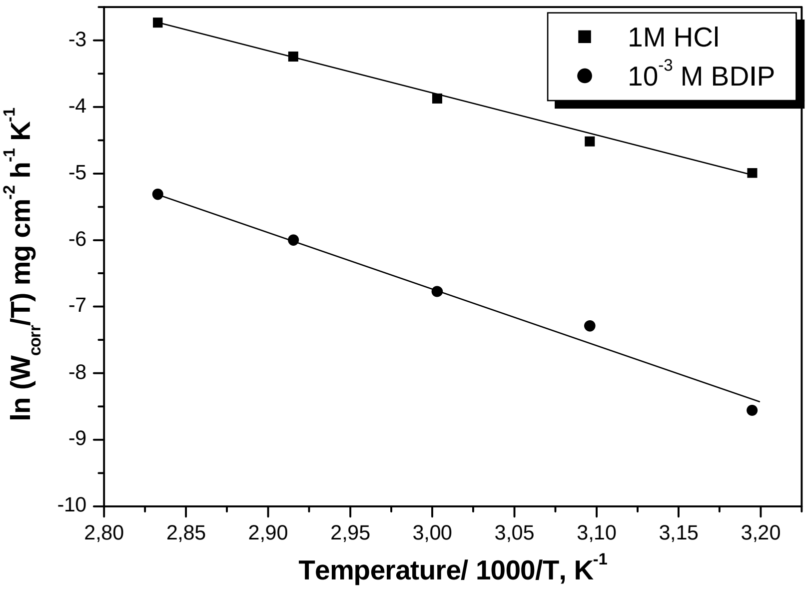

Figure 4: The relation between ln (W_{corr}/T) vs. 1/T for mild steel at 10^{-3} M of BDIP

Table 5 exemplifies the activation parameters of the metal dissolution in the absence and presence of BDIP.

Table 5 The values of activation parameters E_a, ΔH^* and ΔS^* for mild steel in 1 M HCl and added of 10^{-3} M of BDIP

Concentration mol L^{-1}	E_a kJ mol^{-1}	ΔH^* kJ mol^{-1}	ΔS^* J K^{-1} mol^{-1}
Blank	56	53.3	− 69.8
10^{-3}	74.6	71.8	− 38.3

3.5. Adsorption isotherm

Several adsorption isotherms were assessed and the Langmuir adsorption isotherm was found to be the best description of the adsorption behaviour of the studied inhibitor, which obeys to equation (7) [32]:

$$\frac{C_{inh}}{\theta} = \frac{1}{K_{ads}} + C_{inh}, \quad with \quad K_{ads} = \frac{1}{55{,}55}\exp\left(-\frac{\Delta G^{\circ}_{ads}}{RT}\right) \tag{7}$$

C_{inh} is the inhibitor concentration, θ is the fraction of the surface covered, K_{ads} is the adsorption coefficient, and ΔG°_{ads} is the standard free energy of adsorption.

Figure 5 shows the dependence of the ratio of the surface covered C_{inh}/θ as a function of the concentration (C_{inh}) of BDIP. The degree of surface coverage θ at different concentrations of the inhibitor in acidic medium has been evaluated from weight loss using the following equation (8) [33]:

$$\theta = \frac{W_{corr}(\theta = 0) - W_{corr}(\theta)}{W_{corr}(\theta = 0) - W_{corr}(\theta = 1)} \tag{8}$$

Where $W_{corr}(\theta = 0)$ and $W_{corr}(\theta)$ are the values of corrosion weight loss after immersion in solution without and with BDIP, respectively, and $W_{corr}(\theta = 1)$ is the corrosion weight loss giving a maximum inhibition, obtained in our case at 10^{-3} M of BDIP. The values of the surface coverage θ are given in Table 1.

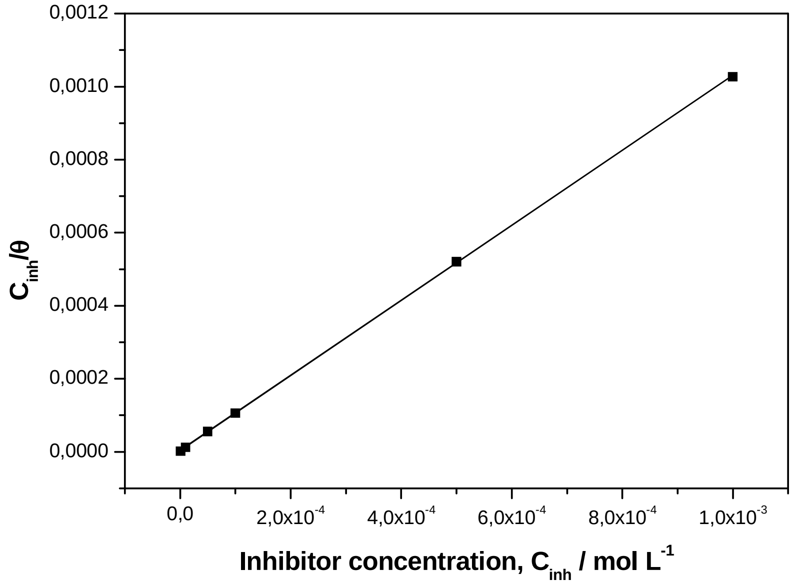

Figure 5: Langmuir isotherm adsorption model of BDIP on the surface of mild steel in 1 M HCl

DISCUSSION

Gravimetric measurements show that the corrosion rate decreases in the presence of BDIP. Its inhibitive action is better expressed by the inhibition efficiency (E_{WL} %), which increases with inhibitor concentration (Table 1) and reaches the maximum value of 97, 4% at 10^{-3} M of BDIP.

The inhibition efficiency of the inhibitors depends on many factors such as the number of adsorption active centres in the molecule and their charge density, molecular size, mode of adsorption, heat of hydrogenation and formation of metallic complex [34]. The higher inhibition efficiency of BDIP may be explained by the presence of nitrogen atoms, π-electrons of pyridine and imidazole rings and methyl's (electron donor groups by inductive effect). The nitrogen atoms are the major adsorption centres because of their interaction with the metal surface [35].

The adsorption of BDIP on the metal surface can occur either directly on the basis of donor–acceptor interactions between the π-electrons of the ring and the vacant d-orbitals of mild steel surface atoms or an interaction of organic nitrogen compounds with already adsorbed groups as proposed in [36,37] and reflected in Scheme 2. Immediately afterwards, as the corrosion reaction starts, ferrous ion may be surrounded by the two imidazolyl nitrogen atoms at Fe—N (2) and Fe—N (4), as well as the nitrogen of the pyridine group Fe—N (3) [38] as proposed in Scheme 3.

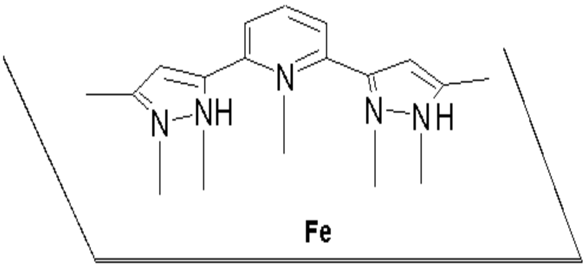

Scheme 2: Schematic representation of the mode of adsorption of BDIP onto the mild steel surface

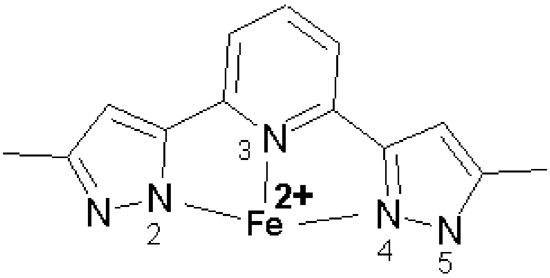

Scheme 3: Complex suggested to be formed on the mild steel surface

From electrochemical polarisation measurements, it is clear from the results that the addition of BDIP causes a decrease of the current density in the cathodic as well as in the anodic branch. These results demonstrate that the hydrogen evolution reaction as well as the iron metal dissolution is inhibited and that the inhibition efficiency increases with inhibitor concentration. The addition of the inhibitor does not change the values of the corrosion potential E_{corr} which allowed that BDIP being of mixed type inhibitor. The i_{corr} values of mild steel in the inhibited solution are smaller than that for the inhibitor free solution (Table 2). The parallel cathodic Tafel plots obtained in Fig. 1 indicate that the hydrogen evolution is activation-controlled. The cathodic Tafel slopes (β_c) change when the concentration increases which suggests that the reduction mechanism is affected by the presence of the BDIP inhibitor. In the anodic range, the polarisation curves of mild steel show that the addition of BDIP decreases the current densities up to E = -300 mV potential; after this potential, the inhibitor doesn't seem to affect the polarization curve, this result shows that the inhibitory action depends on the potential.

From EIS measurements, the presence of BDIP is accompanied by the increase of the value of R_{ct} in acidic solution indicating that a charge transfer process mainly controls the mild steel corrosion. We remark that R_{ct} increases with increasing the inhibitor concentration and E_{imp}% increases to attain 94% at 10^{-3} M. The values of double-layer capacitance are also brought down to the maximum extent in the presence of the BDIP inhibitor and the decrease in the values of C_{dl} follows the order similar to that obtained for i_{corr} in this study. The decrease in C_{dl} can be imputed to the adsorption of the inhibitor on the metal surface leading to the formation of film or complex in acidic solution [39].

It is to be mentioned that the values of inhibition efficiency of the BDIP inhibitor obtained by electrochemical impedance spectroscopy methods are in good agreement and follow the same trend with those obtained from I-E and weight loss measurements.

The effect of temperature shows that the increase of corrosion rate W_{corr} is more pronounced with the rise of temperature for the blank solution than in the presence of BDIP. We note that the efficiency of BDIP (E_{WL} %) very slightly decrease when the temperature rises from 313 to 353 K at 10^{-3} M of BDIP. Accordingly the inhibiting efficiency is circa temperature independent at 10^{-3} M of BDIP inhibitor.

The presence of the BDIP inhibitor causes a change in the values of apparent activation energy. We note also that the addition of the BDIP inhibitor at 10^{-3} M increases the value of the activation energy compared to the blank. This phenomenon is often interpreted by physical adsorption leading to the formation of an adsorptive film of electrostatic character [40]. Beside the fact that the inhibition phenomenon can be imputed to the presence of empty d-orbital in the Fe which led to an easier coordinate bond formation between the metal and inhibitors, these last contain nitrogen atoms which are easily protonated in HCl medium. Therefore, physical adsorption is also possible via electrostatic interaction between a negatively charged surface, which is provided with a specifically adsorbed chloride anion on mild steel, and the positive charge of the BDIP inhibitor [41].

The positive values of ΔH^* mean that the dissolution reaction is an endothermic process and the dissolution of mild steel is difficult [42]. Practically E_a and ΔH^* are the same order. This result enabled us to check the thermodynamic relation of Gomma and Wahdan [43] between E_a and ΔH^* as shown in equation (9):

$$E_a - \Delta H^* = RT \qquad (9)$$

The calculated value of the difference is 2.6 kJ mol^{-1} in the two solutions which is close to the experimental value of *RT*, ca. 2.56 kJ mol^{-1} at 308 K. Also the entropy ΔS^* increases in the presence of BDIP than the non-inhibited one. The increase of ΔS^* in inhibited medium implies that the activation of BDIP in the rate-determining step represents an association rather than dissociation step, meaning an increase in disordering taking place on moving from reactants to activated complex [44].

Figure 6 illustrates the dependence of the fraction of the concentration and the surface covered C_{inh}/θ as a function of the concentration of the BDIP molecule. The obtained plot of the inhibitor is linear with a slope of 1.02 close to unity. The regression coefficient is $r = 0.99998$. The intercept permits the calculation of the equilibrium constant K_{ads} which is 318836 M^{-1} which leads to evaluate $\Delta G°_{ads} = -42.76$ kJ/mol. The negative value of $\Delta G°_{ads}$ indicates that the inhibitor is spontaneously adsorbed on the metal surface [40]. It is well known that the absolute values of $\Delta_{ads}G^0$ of order of 20 kJ mol^{-1} or lower indicate a physisorption; while those of order of 40 kJ mol^{-1} or higher are associated with chemisorption [45]. It is suggested that the adsorption mechanism of the investigated inhibitor on the mild steel surface in 1 M HCl solution involves chemisorption. This is in fact possible in view of the presence of unshared electron pairs in the organic compounds molecules and taking into consideration the behaviour of Fe as electrons acceptor as its d-submonolayer is incomplete. The inhibitor studied may then be adsorbed via donor–acceptor interactions between the π-electrons of the aromatic systems and the unshared electrons pairs of the *-N* heteroatoms to form a bond with the vacant d orbital of the iron atom on the metal surface, which act as a Lewis acid, leading to the formation of a protective chemisorbed film.

CONCLUSION

The following main conclusions are drawn from the present study:

1. The protection efficiency of the BDIP inhibitor under study increases with the increase of the inhibitor concentration.
2. Polarisation measurements show that the BDIP acts as a mixed type inhibitor from -800 mV to -300 mV, and the cathodic curves presented in the Tafel lines indicate that the hydrogen evolution reaction at the metal surface occurs through a pure mechanism of activation.
3. BDIP adsorbs on the mild steel surface according to the Langmuir isotherm adsorption.
4. The weight loss, electrochemical impedance spectroscopy and polarisation curves were in good agreement.
5. It is observed that the inhibiting efficiency remain almost constant at so higher values even at higher temperatures in the presence of 10^{-3} M BDIP which implies chemisorption. In contrast, the higher value of activation energy of the dissolution process compared to that in the free inhibitor solution implies physisorption. The calculated standard free Gibbs energy corresponding to BDIP adsorption process of less than - 40 kJ mol^{-1} is favorable of chemisorption.

It remains not evident to attribute bluntly either chemisorption or physisorption mechanism for the studied inhibitor. The authors believe that the studied inhibitor is adsorbed by mixed mode (physisorption and chemisorption both involved to some extent) onto the mild steel surface.

REFERENCES

[1] H.H. Uhlig and R.W. Revie, Corrosion and Corrosion Control, Wiley, New York (1985).
[2] G. Schmitt, *Br. Corros. J.*, **1984,** 19, 165.
[3] G. Trabanelli In: Florain Mansfeld, Editor, *Chemical Industries: Corrosion Mechanism, Chap. 3: Corrosion Inhibitors 28, 120*, Marcel Dekker, New York (1987).
[4] S. Muralidharan, R. Charasekar and S.V.K. Iyer, *Proc. Indian Acad. Sci., Chem. Sci.*, **2000,** 112, 127.
[5] F. Bentiss, M. Traisnel, M. Lagrenée, *Corros. Sci.* **2000,** 42, 127.
[6] A. Chetouani, A. Aouniti, B. Hammouti, N. Benchat, T. Benhadda, S. Kertit, *Corros. Sci.*, **2003**, 45 1675.
[7] J.G.N. Thomas, Proc 5th European Symposium on Corrosion Inhibitors, *Ann. Univ. Ferrara, N.S. Sez. V.*, **1980,** 8, 453.
[8] A. Aouniti, B. Hammouti, M. Brighli, S. Kertit, F. Berhili, S. El Kadiri, A Ramdani, *J. Chim. Phys.*, **1996,** 93, 1262.
[9] M. Abdallah, M.M. El Naggar, *Mater. Chem. Phys.*, **2001,** 71, 291.
[10] A.G. Gad Allah, H.M. Tamous, *J. Appl. Electrochem.*, **1990,** 20; 488.
[11] A.G. Gad Allah, H. Moustafa, *J. Appl. Electrochem.*, **1992,** 22, 644.
[12] K. Tebbji, H. Oudda, B. Hammouti, M. Benkaddour, M. El Kodadi, F. Malek, Ramdani, *Appl. Surf. Sci.*, **2005,** 241, 326.
[13] F. Touhami, A. Aouniti, S. Kertit, Y. Abed, B. Hammouti, A. Ramdani, K. El Kacemi, *Corros. Sci.* **2000,** 42, 929.

[14] A. Dafali, B. Hammouti, R. Touzani, S. Kertit, A. Ramdani and K. El Kacemi, *Anti-Corros. Methods Mater.,* **2002,** 49, 96.
[15] F. Touhami, B. Hammouti, A. Aouniti, S. Kertit, *Ann. Chim. Sci. Mater.* **1999,** 24 ; 581.
[16] A. El-Ouafi, B. Hammouti, H. Oudda, S. Kertit, R. Touzani, A. Ramdani, *Anti-Corros. Methods Mater.,* **2002,** 49, 199.
[17] K. Tebbji, H. Oudda, B. Hammouti, M. Benkaddour, M. El Kodadi, A. Ramdani, *Colloids Surf., A Physicochem. Eng. Asp.,* **2005,** 259, 157.
[18] M. Elayyachy, M. El Kodadi, B. Hammouti, A. Ramdani, A. El Idrissi, *Pigm. Resin.Technol.,* **2004,** 33, 375.
[19] F. Bentiss, M. Traisnel, L. Gengembre, M. Lagrenée, *Appl. Surf. Sci.,* **2000,** 161, 194.
[20] S. Ramesh, S. Rajeswari, S. Maruthamuthu, *Appl. Surf. Sci.,* **2004,** 229, 214.
[21] A.B. Tadros, B.A. Abdenaby, *J. Electroanal. Chem.,* **1988,** 246, 433.
[22] R. Agrawal, T.K.G. Namboodhiri, *J. Appl. Electrochem.,* **1992,** 22; 383.
[23] G. Xue, J. Ding, P. Lu, J. Dong, *J. Phys. Chem.,* **1991,** 95, 7380.
[24] H.L. Wang, H.B. Fan, J.S. Zheng, *Mater. Chem. Phys.,* **2002,** 77, 655.
[25] M.A. Quraishi, D. Jamal, *Mater. Chem. Phys.,* **2001;** 68, 283.
[26] S. Kertit, B. Hammouti, *Appl. Surf. Sci.,* **1996,** 93, 5966.
[27] S. Kertit, H. Essouffi, B. Hammouti, M. Benkaddour, *J. Chim. Phys.,* **1998,** 95 ; 2072.
[28] S. Kertit, K. Bekkouche, B. Hammouti, *Rev. Metall. Sci. Mater., (Paris)* **1998,** 97, 251.
[29] F. Chaouket, B. Hammouti, S. Kertit and K. El Kacemi, *Bull. Electrochem.,* **2001,** 17 311.
[30] (a) F. Mansfeld, M.W. Kending, S. Tsai, *Corrosion* **1981,** 37; 301. (b) F. Mansfeld, M.W. Kending, S. Tsai, *Corrosion* **1982,** 38, 570.
[31] T. Tsurus, S. Haruyama and B. Gijutsu, *J. Jpn. Soc. Corros. Eng.,* **1978,** 27, 573.
[32] I. Langmuir, *J. Amer. Chem. Soc.,* **1947,** 39, 1848.
[33] D. Landolt, *Corrosion et Chimie de Surface des Métaux* (1st Ed.), Alden Press, Oxford (1993) 495.
[34] S. Fouda, M.N. Moussa, H.F.I. Mtaba, *Corros. Sci.,* **1986,** 26, 719.
[35] N. Nobe, N. Eldakar, *Corrosion* **1981,** 37, 271.
[36] N. Hackerman, E.S. Snavely, J.S. Payne, *J. Electrochem. Soc.,* **1966,** 113, 677.
[37] T. Murakawa, S. Nagaura, N. Hackerman, *Corros. Sci.,* **1967,** 7, 79.
[38] W.-D. Ihlenfeldt, J. Gasteiger, *J. Comput. Chem.,* **1994,** 8, 793.
[39] F. Bentiss, M. Lagrenée, M. Traisnel J.C. Hornez, *Corros. Sci.,* **1999,** 41, 789.
[40] A. Popova, E. Sokolova, S. Raicheva, M. Chritov, *Corros. Sci.,* **2003,** 45, 33.
[41] Y. Feng, K.S. Siow, W.K. Teo, A.K. Hsieh, *Corros. Sci.,* **1999,** 41, 829.
[42] M. Bouklah, N. Benchat, B. Hammouti, A. Aouniti, S. Kertit, *Corros. Sci.,* **2006,** 60, 1904.
[43] G.K. Gomma, M.H. Wahdan, *Mater. Chem. Phys.,* **1995,** 39, 209.
[44] I. El Ouali, B. Hammouti, A. Aouniti, Y. Ramli, M. Azougagh, E.M. Essassi, M. Bouachrine, *J. Mater. Environ. Sci.* **2010,** 1, 1.
[45] J. Wang, C. Cao, J. Chen, M. Zhang, G. Ye, H. Lin, *J. Chin. Soc. Corros. Protec.,* **1995,** 15, 241.